AMERICAN SOCIETY FOR MICROBIOLOGY | mBio®

RESEARCH ARTICLE

In Vivo-Selected Compensatory Mutations Restore the Fitness Cost of Mosaic *penA* Alleles That Confer Ceftriaxone Resistance in *Neisseria gonorrhoeae*

Leah R. Vincent,[a]* Samuel R. Kerr,[b]* Yang Tan,[b] Joshua Tomberg,[b] Erica L. Raterman,[a] Julie C. Dunning Hotopp,[c] Magnus Unemo,[d] Robert A. Nicholas,[b,e] Ann E. Jerse[a]

[a]Department of Microbiology and Immunology, F. Edward Hébert School of Medicine, Uniformed Services University, Bethesda, Maryland, USA

[b]Department of Pharmacology, University of North Carolina at Chapel Hill, Chapel Hill, North Carolina, USA

[c]Department of Microbiology and Immunology, Institute for Genome Sciences, University of Maryland School of Medicine, Baltimore, Maryland, USA

[d]World Health Organization Collaborating Centre for Gonorrhoea and Other Sexually Transmitted Infections, Swedish Reference Laboratory for Sexually Transmitted Infections, Department of Laboratory Medicine, Microbiology, Faculty of Medicine and Health, Örebro University, Örebro, Sweden

[e]Department of Microbiology and Immunology, University of North Carolina at Chapel Hill, Chapel Hill, North Carolina, USA

ABSTRACT Resistance to ceftriaxone in *Neisseria gonorrhoeae* is mainly conferred by mosaic *penA* alleles that encode penicillin-binding protein 2 (PBP2) variants with markedly lower rates of acylation by ceftriaxone. To assess the impact of these mosaic *penA* alleles on gonococcal fitness, we introduced the mosaic *penA* alleles from two ceftriaxone-resistant (Cro^r) clinical isolates (H041 and F89) into a Cro^s strain (FA19) by allelic exchange and showed that the resultant Cro^r mutants were significantly outcompeted by the Cro^s parent strain *in vitro* and in a murine infection model. Four Cro^r compensatory mutants of FA19 *penA41* were isolated independently from mice that outcompeted the parent strain both *in vitro* and *in vivo*. One of these compensatory mutants (LV41C) displayed a unique growth profile, with rapid log growth followed by a sharp plateau/gradual decline at stationary phase. Genome sequencing of LV41C revealed a mutation (G348D) in the *acnB* gene encoding the bifunctional aconitate hydratase 2/2 methylisocitrate dehydratase. Introduction of the $acnB_{G348D}$ allele into FA19 *penA41* conferred both a growth profile that phenocopied that of LV41C and a fitness advantage, although not as strongly as that exhibited by the original compensatory mutant, suggesting the existence of additional compensatory mutations. The mutant aconitase appears to be a functional knockout with lower activity and expression than wild-type aconitase. Transcriptome sequencing (RNA-seq) analysis of FA19 *penA41* $acnB_{G348D}$ revealed a large set of upregulated genes involved in carbon and energy metabolism. We conclude that compensatory mutations can be selected in Cro^r gonococcal strains that increase metabolism to ameliorate their fitness deficit.

IMPORTANCE The emergence of ceftriaxone-resistant (Cro^r) *Neisseria gonorrhoeae* has led to the looming threat of untreatable gonorrhea. Whether Cro resistance is likely to spread can be predicted from studies that compare the relative fitnesses of susceptible and resistant strains that differ only in the *penA* gene that confers Cro resistance. We showed that mosaic *penA* alleles found in Cro^r clinical isolates are outcompeted by the Cro^s parent strain *in vitro* and *in vivo* but that compensatory mutations that allow ceftriaxone resistance to be maintained by increasing bacterial fitness are selected during mouse infection. One compensatory mutant that was studied in more detail had a mutation in *acnB*, which encodes the aconitase that

Received 18 October 2017 **Accepted** 20 February 2018 **Published** 3 April 2018

Citation Vincent LR, Kerr SR, Tan Y, Tomberg J, Raterman EL, Dunning Hotopp JC, Unemo M, Nicholas RA, Jerse AE. 2018. *In vivo*-selected compensatory mutations restore the fitness cost of mosaic *penA* alleles that confer ceftriaxone resistance in *Neisseria gonorrhoeae*. mBio 9:e01905-17. https://doi.org/10.1128/mBio.01905-17.

Editor Michael S. Gilmore, Harvard Medical School

Address correspondence to Robert A. Nicholas, nicholas@med.unc.edu, or Ann E. Jerse, ann.jerse1@usuhs.edu.

* Present address: Leah R. Vincent, NIAID, Bethesda, Maryland, USA; Samuel R. Kerr, Yale University, New Haven, Connecticut, USA.

functions in the tricarboxylic acid (TCA) cycle. This study illustrates that compensatory mutations can be selected during infection, which we hypothesize may allow the spread of Cro resistance in nature. This study also provides novel insights into gonococcal metabolism and physiology.

KEYWORDS *Neisseria gonorrhoeae*, aconitase, antibiotic resistance, biological fitness, competitive index

Neisseria gonorrhoeae is the etiologic agent of the sexually transmitted infection gonorrhea. An estimated 78 million gonococcal infections occur worldwide per year, and the associated morbidity and mortality take a significant toll on public health (1). A high percentage of cervical, rectal, and pharyngeal infections in both men and women are asymptomatic, which contributes to the spread of infection (2). More serious infections occur when the gonococcus ascends to the upper reproductive tract, where it can cause epididymitis or pelvic inflammatory disease (PID), along with the associated sequelae of chronic pelvic pain, ectopic pregnancy, and infertility. Maternal gonorrhea can lead to multiple complications during pregnancy and birth, including premature rupture of membranes, low-birth weight, and neonatal conjunctivitis, the last of which can lead to corneal scarring and blindness (2). Gonococcal infections increase the risks of acquiring and transmitting HIV (3, 4). Because there is no effective gonorrhea vaccine, antibiotic treatment of infected individuals and their sexual contacts is a critical control measure for these infections.

This public health strategy is constantly challenged by the inexorable evolution of antibiotic resistance in *N. gonorrhoeae* (5), which causes relatively frequent changes in treatment recommendations and a substantial investment of public health funds in global surveillance programs, prevention strategies, and diagnostics (6). Gonococcal resistance to penicillin, tetracycline, and early macrolide antibiotics rose to unacceptable levels by the 1980s. These antibiotics were replaced as the recommended empirical treatments for gonorrhea by fluoroquinolones and extended-spectrum cephalosporins (ESCs) (5). However, the rapid emergence of fluoroquinolone-resistant strains, which is due to mutations in the topoisomerase subunit genes *gyrA* and *parC*, resulted in the removal of fluoroquinolones from the list of recommended first-line therapies for gonorrhea in 2007 in the United States and even earlier in Europe and Asia, leaving only the ESCs, specifically cefixime and ceftriaxone (Cro), as the last remaining options for monotherapy (5, 7). Alarmingly, decreasing susceptibility and emergence of resistance to the ESCs, particularly cefixime, led to the removal of cefixime as a recommended antibiotic, a change to dual therapy, and the elevation of the gonococcus to "superbug" status (5, 8, 9). The first documented high-level ceftriaxone-resistant (Cro^r) strain, H041, was isolated from a pharyngeal infection of a sex worker in Kyoto, Japan, in 2009 (10, 11). This report was followed by the emergence of the high-level Cro^r strain F89 in France and its documented transmission between two male sexual partners in Spain (12, 13). Both H041 and F89 are resistant to the majority of antibiotics used to treat gonorrhea (10, 12).

Resistance to ESCs in *N. gonorrhoeae* is chromosomally mediated and occurs through the stepwise acquisition of at least three resistance determinants: *penA*, which encodes a mosaic variant of penicillin-binding protein 2 (PBP2) that functions during cell division (14–16); *mtrR*, which encodes mutations in the MtrR repressor or mutations in the overlapping promoters of *mtrR* and *mtrCDE* that increase expression of the MtrC-MtrD-MtrE efflux pump (15, 17); and *penB*, which encodes mutations in the outer membrane porin, PorB1b, that decrease the influx of antibiotics into the periplasmic space (18–20). While all of the abovementioned resistance determinants contribute to ESC resistance, remodeling of the lethal target of the ESCs, PBP2, is the most important (15). Indeed, the mosaic *penA* alleles from either H041 or F89, when introduced into an antibiotic-susceptible strain, are sufficient to confer ceftriaxone resistance on their own (10, 12, 21). Mosaic *penA* alleles encode altered PBP2 variants with up to 63 amino acid substitutions that arise from multiple recombination events between the gonococcal

penA gene and *penA* alleles from commensal and pathogenic *Neisseria* species (*N. sicca*, *N. cinerea*, *N. perflava*, *N. flavescens*, and *N. meningitidis*) (14). The ESCs are substrate analogs of the C-terminal acyl-D-Ala-D-Ala peptide chain of peptidoglycan that kill bacteria by covalently inhibiting the PBP transpeptidases that cross-link peptidoglycan. The mosaic variants of PBP2 from H041 and F89 display marked decreases (2,000- to 10,000-fold) in the second-order rate constants (k_2/K_S) for acylation by ESCs, highlighting the remarkable remodeling of PBP2 to exclude substrate analogs (β-lactam antibiotics) while retaining sufficient essential transpeptidase activity to support cell viability (21–23).

Antibiotic resistance mutations can impact bacterial fitness by conferring a fitness cost or benefit in the absence of antibiotic pressure (24). It is not known whether acquisition of the mosaic *penA* alleles from H041 or F89 is accompanied by a fitness cost. We previously showed that resistance mutations in *gyrA* and the *mtrR* gene or its promoter increase *N. gonorrhoeae* fitness *in vivo* but not *in vitro* (25, 26). *mtrR* mutations are likely to increase fitness due to overproduction of the MtrC-MtrD-MtrE efflux pump, which protects the gonococcus from innate antimicrobial effectors (25). The basis of the fitness advantage conferred by *gyrA* mutations (S91F/D95N) is unknown but may be a consequence of global changes in gene expression (27). In contrast to *mtrR* and *gyrA* mutations, PBP mutations that confer resistance to β-lactams are predicted to have a negative impact on gonococcal fitness based on fitness studies in Gram-positive organisms (28–30) and the importance of these enzymes in cell wall biosynthesis. In *N. gonorrhoeae*, however, this prediction runs counter to surveillance data showing that strains with some mosaic *penA* alleles are prevalent (31); one way in which these strains could flourish, even in the absence of antibiotic selection, is to acquire spontaneous compensatory mutations that ameliorate this defect (32). In support of this hypothesis, we previously showed that whereas acquisition of multiple resistance mutations ($gyrA_{91/95}$, $parC_{86}$, and mtr_{-79}) or insertional inactivation of the *mtrCDE* activator gene, *mtrA*, significantly compromised the capacity of *N. gonorrhoeae* to grow *in vitro* and establish infection in female mice, one or more compensatory mutations were selected during murine infection that restored fitness to these mutants without compromising resistance levels (26, 33).

In this study, we tested the hypothesis that mosaic *penA* alleles that confer high-level Cro resistance decrease the fitness of *N. gonorrhoeae* and that compensatory mutations could arise to alleviate this fitness defect(s). We constructed strains in the Cro^s FA19 strain background that harbor the mosaic *penA41* or *penA89* allele from Cro^r clinical isolate H041 or F89, respectively. We then measured the relative fitness of these strains by competitive coculture in broth and competitive coinfections of female mice. We isolated four compensatory Cro^r mutants from murine infections with increased fitness, and the genomes of these mutants were sequenced. One of these strains contained a mutation in the bifunctional aconitate hydratase 2/2 methylisocitrate dehydratase enzyme that functions in the tricarboxylic acid (TCA) cycle. The consequence of this mutation for bacterial growth *in vitro*, *in vivo* fitness in the murine model of gonococcal infection, and global gene transcription when expressed in a Cro^r strain background was investigated, and our results indicate that one potential mechanism to increase fitness of Cro^r strains is to increase cellular metabolism.

RESULTS

Mosaic *penA41* and *penA89* alleles reduce gonococcal fitness *in vitro*. To assess the impact of mosaic *penA* alleles that confer ESC resistance on fitness, we transformed the mosaic *penA* allele from the Cro^r strains H041 and F89 into strain FA19, resulting in strains FA19 *penA41* and FA19 *penA89*, respectively (see Table S1 in the supplemental material). Importantly, the FA19 strain that we used in this study has a single missense mutation in the *rpsL* gene that confers streptomycin resistance, which is critical for use in the mouse infection model (Table S1). The MIC of Cro for FA19 *penA41* and FA19 *penA89* was 500-fold higher than that for the parental strain (MICs of 0.5 μg/ml versus 0.001 μg/ml for FA19). We hypothesized that the presumed decrease in essential

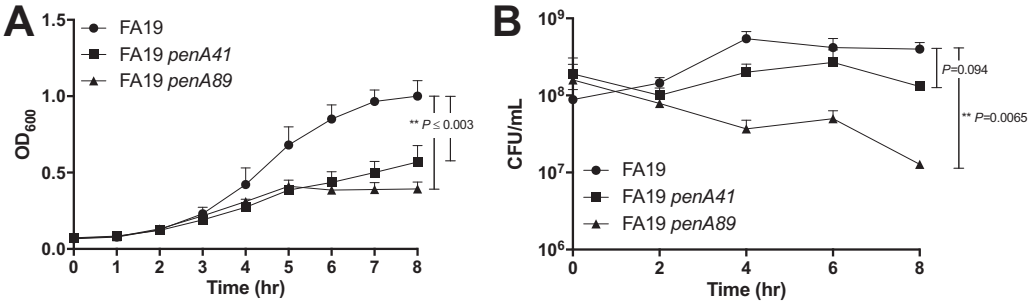

FIG 1 The mosaic *penA41* and *penA89* alleles negatively affected growth of the Cro^s wild-type FA19 parental strain. Strains were grown over an 8-h period with agitation at 220 rpm and 37°C. (A) Optical density at 600 nm (OD_{600}) measured at hourly intervals. (B) CFU per milliliter measured at 2-h intervals. Results are combined data from three independent experiments for each strain. Error bars show the standard errors of the means (SEM). Statistical significance was calculated using a repeated-measures 2-way ANOVA with Tukey's multiple comparisons. *P* values shown are for each mutant strain versus FA19.

transpeptidase activity caused by the extensive remodeling of PBP2 would impair bacterial growth (21, 23). To test this hypothesis, strains FA19, FA19 *penA41*, and FA19 *penA89* were cultured independently in liquid GC medium broth (GCB). Growth of the mutant strains was clearly impaired as evidenced by decreases in both optical density (Fig. 1A) and the number of viable bacteria recovered (Fig. 1B) over time, with strain FA19 *penA89* exhibiting the most pronounced fitness cost.

We next measured the capacity of the Cro^s parental strain to outcompete the Cro^r strains by performing cocultures in GCB under standard growth conditions. FA19 *penA41* bacteria were consistently less fit than FA19 as shown by 10-fold and 50-fold decreases in the relative number of Cro^r gonococci recovered after 6 and 8 h of growth, respectively (Fig. 2A; Table 1). As predicted from the noncompetitive cultures, FA19 *penA89* showed a more pronounced fitness defect, with growth decreased 17-fold relative to FA19 within the first 4 h of incubation and 330-fold at 8 h (Fig. 2B). We conclude that these mosaic *penA* alleles are detrimental to gonococcal growth *in vitro*, with the *penA89* allele being the most attenuating.

Mosaic *penA41* and *penA89* alleles reduce *in vivo* fitness in the murine model, but compensatory mutant strains can be selected during infection. To determine whether the fitness disadvantages observed *in vitro* also occur *in vivo*, we carried out competitive infections in the murine model of gonococcal genital tract infection (34). BALB/c mice were inoculated vaginally with similar numbers of FA19 and either FA19 *penA41* or FA19 *penA89*, and the CFU of each strain isolated from vaginal swabs were determined over 7 days. Overall, fewer mutant bacteria were recovered from mice relative to the parental strain over the course of infection. When the ratio of the two strains in the inoculum was compared to the ratio of each strain in vaginal cultures (expressed as a competitive index [CI]), FA19 *penA41* showed reduced fitness relative to FA19 with a 2.9-fold decrease in the mean CI on day 1 and a 4.3-fold decrease on day 3 (Fig. 2C). No Cro^r CFU were recovered from 4/9 mice infected with FA19 and FA19 *penA41* on day 5 (Fig. 2C, open triangles). In contrast, FA19 *penA89* was severely outcompeted by FA19 as shown by a 50-fold decrease on day 1 and a $>$10,000-fold decrease in fitness on all other culture days (Fig. 2D). Indeed, no Cro^r CFU were recovered after day 1 (Fig. 2D, open triangles), whereas 5×10^3 to $>1 \times 10^5$ CFU of FA19 were recovered at the final time point.

Interestingly, and in contrast to experiments with FA19 *penA89*, we detected an upward shift in the CI in five of nine mice inoculated with FA19 and FA19 *penA41* after an earlier decrease in the CI (Fig. 2C; CI values that showed this shift are indicated by †). In some cases, Cro^r bacteria completely outcompeted the Cro^s strain (Fig. 2C, open circles). We suspected that these bacteria had acquired spontaneously occurring compensatory mutations that improved fitness during infection in these mice, and we made frozen stocks of well-isolated single colonies from Cro-containing agar plates. Four of

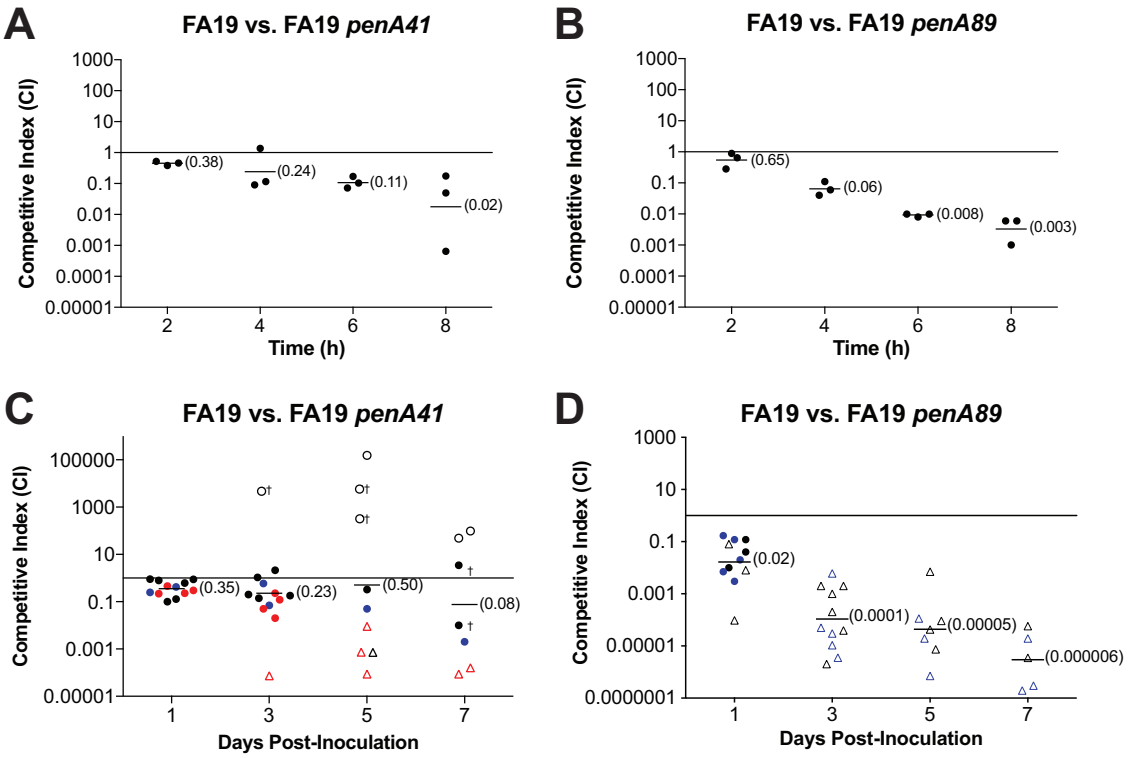

FIG 2 The mosaic *penA41* and *penA89* alleles conferred a fitness disadvantage both *in vitro* and *in vivo*, but compensatory mutants of strain FA19 *penA41* can be selected during infection. (A and B) Broth cultures were inoculated with similar numbers of wild-type FA19 and either FA19 *penA41* (A) or FA19 *penA89* (B). The competitive index (CI) was determined in early, mid-log, and late log stages by dividing the ratio of mutant to wild-type bacteria at output by the ratio of mutant to wild-type bacteria at input. (C and D) Female BALB/c mice were inoculated vaginally with similar numbers of wild-type FA19 and either FA19 *penA41* (C) or FA19 *penA89* (D). The CI was determined as described for panels A and B. Each symbol indicates the CI for an individual mouse, and colors indicate separate experiments. The horizontal bars indicate the geometric mean (also shown in parentheses), and the solid line indicates a competitive index of 1. Open circles in panels C and D indicate mice from which only Cro^r CFU were recovered, while open triangles indicate mice from which only Cro^s CFU were recovered. For those cultures, the limit of detection (4 CFU) was used as the number of CFU for the strain that was not isolated when calculating the CI. Dagger symbols correspond to mice from which putative compensatory mutants were observed. Isolates from these mice were frozen for further analysis. Data from three independent experiments are shown.

these putative mutant strains, LV41A, LV41B, LV41C, and LV41E, were subjected to further phenotypic and genotypic analyses.

MICs and growth characteristics of compensatory mutant strains *in vitro*. The MICs of Cro for LV41A, LV41B, LV41C, and LV41E were unchanged from that for the FA19 *penA41* parent strain (0.5 μg/ml). We also determined the MICs of ciprofloxacin and erythromycin because mutations in one of the targets of ciprofloxacin (*gyrA*), or mutations in the *mtrR* gene that increase the MIC of erythromycin, alter *in vivo* fitness

TABLE 1 *In vitro* growth kinetics of compensatory mutant strains compared to Cro^s and Cro^r parent strains

Bacterial strain	Time (min) to reach OD_{600} of 0.8 ± SE	*P* value for strain vs[a]: FA19	FA19 *penA41*
FA19	205.2 ± 3.7		0.001[c]
FA19 *penA41*	278.3 ± 15.6	0.001[b]	
LV41A	233.3 ± 3.3	0.0002[b]	0.018[c]
LV41B	262.5 ± 13.5	0.002[b]	0.461
LV41C	214.0 ± 6.4	0.260	0.003[c]
LV41E	200.0 ± 3.2	0.317	0.0006[c]

[a]Overall significance was determined by a one-way analysis of variance, followed by Student's *t* test to determine significance between individual strains.
[b]Growth is significantly slower than Cro^s strain FA19.
[c]Growth is significantly faster than Cro^r strain FA19 *penA41*.

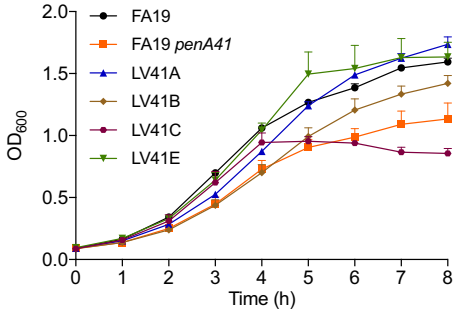

FIG 3 Growth kinetics of the four compensatory mutants compared to the Cro^r and Cro^s parent strains. Bacteria were grown over an 8-h period at 37°C with agitation. The average OD_{600} from six independent experiments is plotted versus time of incubation. The error bars represent the SEM. Statistical significance was calculated using a repeated-measures 2-way ANOVA with Tukey's multiple comparisons. Compensatory mutants LV41A and LV41E grew significantly faster than the Cro^r parent strain FA19 *penA41* ($P <$ 0.001), and the rate was equal to that of the Cro^s strain FA19. Compensatory mutants LV41B and LV41C grew significantly slower than the Cro^s strain FA19 ($P <$ 0.068 and $<$ 0.001, respectively), but there was no statistical difference from the Cro^r parent strain FA19 *penA41*.

(26, 33). There were no differences in the MIC of erythromycin (0.38 μg/ml) or ciprofloxacin (0.03 μg/ml) for the compensatory mutant strains compared to that for FA19 *penA41*, suggesting that mutations in these genes were not responsible for the *in vivo* compensatory phenotype.

To examine the growth characteristics of the *in vivo*-selected mutant strains, we first performed noncompetitive growth curves in GC broth (Fig. 3). Mutant strains LV41A and LV41E grew significantly faster than the Cro^r parent strain, FA19 *penA41*, but similarly to the Cro^s strain, FA19. Compensatory mutant strains LV41B and LV41C grew significantly slower than FA19 but equally as well as FA19 *penA41*. Notably, mutant strain LV41C exhibited a unique growth profile characterized by a rapid log phase, followed by a sharp plateau and gradual decline in values of optical density at 600 nm (OD_{600}). Comparing the times that it took to reach the late log phase, LV41A, LV41C, and LV41E reached an OD_{600} of 0.8 significantly faster than FA19 *penA41* (Table 1), whereas LV41B showed no statistical difference in the time that it took to reach late log phase compared to FA19 *penA41*. These data suggest that the *in vivo*-selected mutation(s) in strains LV41A, LV41C, and LV41E may confer a growth advantage that can compensate for the fitness defect caused by the *penA41* allele and that the mutation in strain LV41C is distinct from the other two in that it promotes rapid growth that is not sustained during stationary phase. Compared to FA19, FA19 *penA41*, LV41A, and LV41B grew significantly more slowly than FA19 (Table 1). In contrast, growth of mutant strains LV41C and LV41E was similar to that of FA19.

We also competed each compensatory mutant against the parental strain FA19 *penA41* or the Cro^s wild-type strain FA19, and the results were as predicted from the noncompetitive growth curves (Table 2). Mutants LV41A and LV41E exhibited a strong

TABLE 2 *In vivo* and *in vitro* CIs for compensatory mutant strains versus Cro^s or Cro^r parent strains

	Fitness relative to that of strain[b]:			
	FA19		FA19 *penA41 cat*	
Bacterial strain	*In vitro* CI	*In vivo* CI	*In vitro* CI	*In vivo* CI
FA19 *penA41*	0.07	0.08	NA[a]	1.0
LV41A	1.0	3.6	6.8	871.0
LV41B	0.2	0.4	1.8	480.0
LV41C	0.6	2.3	1.8	392.0
LV41E	1.0	2.0	16.4	277.0

[a]Respective strain mixture was not tested competitively and is marked as not applicable (NA).
[b]Values represent the mean CI for two *in vivo* competition experiments and three competitive cocultures for each set of strains competed. *In vivo* CIs are from day 7 of infection.

TABLE 3 Nucleotide changes relative to FA19 *penA41* identified in compensatory mutants

Bacterial strain	Genome position	Gene name	Mutation[b]	Annotation/location
LV41A	1849152	*mleN*	ΔAla467[a]	Malate/Na^+-lactate antiporter
	2115410		SNP T→G	Intergenic region 135 bp downstream of *ftsY*
	1849145		SNP G→A	Intergenic region 142 bp downstream of *ftsY*
LV41B	2115410	*mleN*	ΔAla467	Malic/Na^+-lactate antiporter
	1849145		SNP T→G	Intergenic region 135 bp downstream of *ftsY*
	1849152		SNP G→A	Intergenic region 142 bp downstream of *ftsY*
LV41C	964470	*acnB*	SNP Gly348Asp	Aconitate hydratase 2/2 methylisocitrate dehydratase
	2065357	*pglG*	G insertion that puts gene back in frame	Hypothetical protein related to glycosyltransferase-1
	1849145		SNP T→G	Intergenic region 135 bp downstream of *ftsY*
LV41E	1405383		Deletion of A	Promoter region of putative autotransporter
	1849201		SNP C→T	Intergenic region 190 bp downstream of *ftsY*

[a]Δ refers to a codon deletion.
[b]Mutations in silent *pilE* alleles are not included.

fitness advantage relative to FA19 *penA41* but were equally as fit as FA19. In contrast, LV41B showed a slight (1.8-fold) fitness advantage over FA19 *penA41* but was 5-fold less fit than FA19. LV41C was slightly more fit (1.8-fold) than parent strain FA19 *penA41* and slightly less fit (1.7-fold) than FA19. These results suggest that the compensatory mutations in LV41A and LV41E can restore the growth of FA19 *penA41* close to or equal to that of FA19, while those in LV41B can outcompete FA19 *penA41* but not FA19.

Competitive coinfections of *in vivo*-selected compensatory mutants with FA19 *penA41* or FA19. To determine whether the compensatory mutant strains displayed increased fitness *in vivo*, we performed competitive murine infections. Each of the compensatory mutant strains showed a dramatic fitness advantage *in vivo* against FA19 *penA41*, with CIs reflecting a 277- to 871-fold increase in fitness (Table 2). Three of the mutants, LV41A, LV41C, and LV41E, but not LV41B, also outcompeted FA19, albeit not as dramatically, with 2- to 4-fold increases in fitness detected by day 7 of infection relative to FA19 (Table 2). In summary, these studies confirmed the compensatory *in vivo* phenotype for all four mutants; three of the mutants showed increased growth *in vitro* relative to the parental strain, while one mutant, LV41B, has a strong fitness advantage *in vivo* that is not correlated with a growth advantage *in vitro*.

Identification of mutations in the compensatory mutants. To identify the mutation(s) in the compensatory mutants that might be responsible for their increased fitness, we sequenced the genomes of FA19, FA19 *penA41*, and the four compensatory mutant strains and identified the sequence differences relative to the parental strain FA19 *penA41* (Table 3). As expected, the *rpsL* mutation conferring streptomycin resistance was identified in our strain of FA19, FA19 *penA41*, and all of the compensatory mutant strains. Likewise, changes in the sequence of the *penA* gene were identified in each of the resistant strains and were identical in all of the compensatory mutants and FA19 *penA41*. We also observed single nucleotide polymorphisms (SNPs) in multiple silent pilin alleles, which were anticipated based on the antigenic variability of the *pilE* gene, and in the common 3′ region between *ftsY* and *pilE1_2*, which may have arisen as a consequence of recombination at the *pilE1_2* locus. In addition, LV41A and LV41B harbored a codon deletion mutation in *mleN*, which encodes a putative malate/Na^+/lactate antiporter (35). LV41C had an SNP in the *acnB* gene, which encodes the bifunctional aconitate hydratase 2/2 methylisocitrate dehydratase enzyme that reversibly converts citrate to isocitrate in the TCA cycle, and a frameshift mutation in *pglG*, a glycosyltransferase (36). Unexpectedly, LV41E had no coding sequence mutations compared to FA19 *penA41* but did have an A deletion in the promoter region of a putative autotransporter. All of the mutations in protein-encoding genes identified by whole-genome sequencing were confirmed by PCR amplification of genomic DNA and conventional Sanger sequencing.

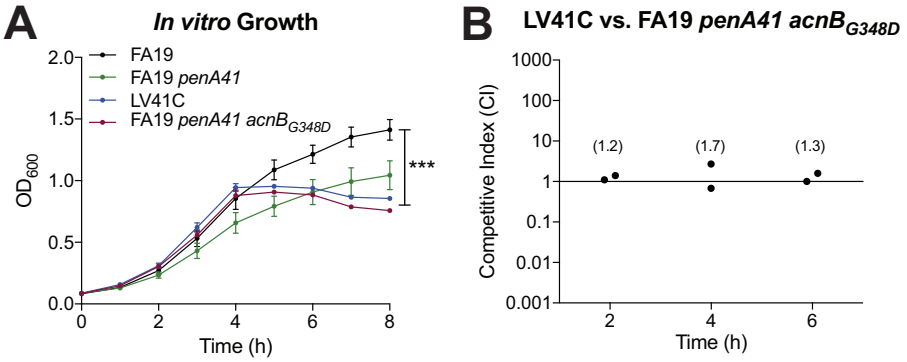

FIG 4 *In vitro* growth phenotype of FA19 *penA41* $acnB_{G348D}$. (A) Noncompetitive growth curves for strains FA19, FA19 *penA41*, LV41C, and FA19 *penA41* $acnB_{G348D}$. (B) Competitive cocultures inoculated with similar numbers of LV41C and FA19 *penA41* $acnB_{G348D}$. The number of CFU of each strain was determined at 2, 4, and 6 h. Data from two independent experiments are shown at each time point, with the mean competitive indexes (CIs) shown in parentheses. Statistical significance was calculated using a repeated-measures 2-way ANOVA with Tukey's multiple comparisons. ***, *P* value ≤ 0.005 of LV41C or FA19 *penA41* $acnB_{G348D}$ compared to FA19.

While there were several mutations to pursue, we chose to focus on the *acnB* mutation in LV41C in this study for several reasons. First, the growth curve of LV41C was both unusual and distinctive (rapid initial growth followed by a sharp plateau/gradual decline). Second, *acnB* is a well-studied enzyme in the TCA cycle and is amenable to enzymatic analysis, and the mutation changing Gly348 to Asp has not been described. Last, changes in metabolism to compensate for a growth defect are an obvious avenue to increase the fitness of Cro^r strains.

Introduction of the $acnB_{G348D}$ allele into FA19 *penA41* and FA19 *penA89* confers increased fitness relative to their respective resistant parental strains. To determine whether the mutated *acnB* allele was responsible for the unusual *in vitro* growth phenotype and *in vivo* fitness differences of the LV41C mutant, we introduced the $acnB_{G348D}$ allele (linked to a downstream kanamycin resistance [Kan^r] cassette for selection) into both the Cro^s strain FA19 and the Cro^r parental strain FA19 *penA41*. The *in vitro* growth profiles of LV41C and FA19 *penA41* $acnB_{G348D}$ were nearly identical, with both strains showing a rapid log phase followed by an early plateau (Fig. 4A). Competitive growth assays with LV41C and FA19 *penA41* $acnB_{G348D}$ showed that the two strains were equally fit through 6 h of growth (Fig. 4B). These data demonstrate that the $acnB_{G348D}$ allele is both necessary and sufficient for the unusual growth phenotype of LV41C.

We next assessed whether the $acnB_{G348D}$ allele increased the fitness of FA19 *penA41* *in vivo* compared to the isogenic parental strain. FA19 *penA41* $acnB_{G348D}$ exhibited a strong fitness advantage early in infection (18- to 76-fold), whereas a 6-fold increase relative to FA19 *penA41* was detected on day 7 of infection; only FA19 *penA41* $acnB_{G348D}$ bacteria were recovered from 3 of 7 infected mice at the latter time point (Fig. 5A). This result was in contrast to LV41C, which exhibited a much greater fitness advantage (400-fold on day 7 of infection) relative to FA19 *penA41* (Table 2). No clear fitness difference was observed when FA19 *penA41* $acnB_{G348D}$ was competed against FA19 (Fig. 5B); in contrast, LV41C was ~3-fold more fit than FA19 by day 7 of infection (Table 2). To confirm that LV41C had a greater fitness advantage than FA19 *penA41* $acnB_{G348D}$, we conducted competitive infections with these two strains, and LV41C clearly outcompeted strain FA19 *penA41* $acnB_{G348D}$ (Fig. 5C).

We also introduced the $acnB_{G348D}$ allele into strains FA19 and FA19 *penA89*. Introduction of the mutated *acnB* allele into strain FA19 resulted in a growth phenotype similar to that shown by FA19 *penA41 acnB* and LV41C (Fig. S1). Strain FA19 *penA89* $acnB_{G348D}$ outcompeted FA19 *penA89* as evidenced by an ~50-fold to >100-fold increase in CIs over the course of infection and the isolation of only FA19 *penA89*

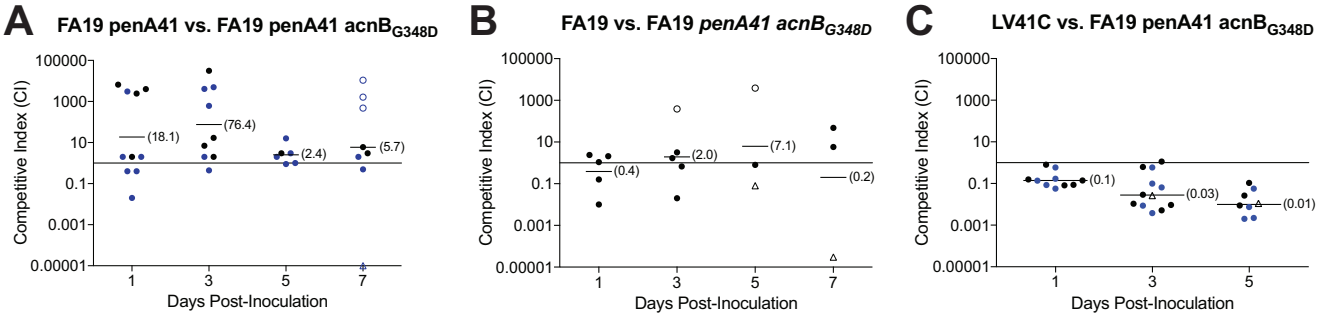

FIG 5 The *acnB*$_{G348D}$ mutation increased the *in vivo* fitness of FA19 *penA41* but not to the same level as the compensatory mutant LV41C. Mice were inoculated vaginally with similar numbers of FA19 *penA41* and FA19 *penA41 acnB*$_{G348D}$ (A), FA19 and FA19 *penA41 acnB*$_{G348D}$ (B), or LV41C and FA19 *penA41 acnB*$_{G348D}$ (C). The ratio of each strain isolated from vaginal swabs was determined, and the CIs for individual mice at each time point were calculated as described for Fig. 2. Open circles indicate that only mutant bacteria were recovered, and open triangles indicate that only the comparative strain was recovered. For those cultures, the limit of detection (4 CFU) was used as the number of CFU for the strain that was not isolated when calculating the CI. The results are combined data from two independent experiments (A and C) or one experiment (B). The bar indicates the geometric mean, which is also indicated by the value in parentheses. Significant differences in the log CIs were found when competing FA19 *penA41 acnB*$_{G348D}$ with FA19 *penA41* (A) compared to FA19 *penA41 acnB*$_{G348D}$ competed against mutant LV41C (C), with *P* values of 0.02, 0.0003, and 0.003 on days 1, 3, and 5, respectively. Day 7 cultures were not collected from mice infected with a mixture of LV41C and FA19 *penA41 acnB*$_{G348D}$.

acnB$_{G348D}$ bacteria from ~50% of mice at each time point (Fig. S2A). We also competed FA19 *penA89 acnB*$_{G348D}$ against FA19, and while the Cro^s strain outcompeted the mutant at every time point (Fig. S2B), the degree of fitness disadvantage exhibited by FA19 *penA89 acnB*$_{G348D}$ was not nearly as severe as that exhibited by FA19 *penA89*, which was unable to survive to day 3 of infection in earlier competition experiments with FA19 (Fig. 2D). Thus, although the *acnB*$_{G348D}$ mutation did not restore the fitness of the highly attenuated strain FA19 *penA89* to the level of the Cro^s wild-type strain, it did partially rescue the *in vivo* fitness defect of strain FA19 *penA89*, a finding that further supports the capacity of this mutation to increase gonococcal growth or survival *in vivo*.

Based on the greater fitness advantage of LV41C over FA19 *penA41 acnB*$_{G348D}$, we tested whether the additional frameshift mutation that restores the open reading frame of the *pglG* gene in LV41C also contributed to fitness *in vivo*. We constructed FA19 *penA41 acnB*$_{G348D}$ *pglG*$^{\text{in-frame}}$ and LV41C *pglG*$^{\text{frame-shift}}$ and conducted competitive infections with LV41C. The results showed that harboring an in-frame *pglG* gene did not alter fitness *in vivo* (Fig. S3).

***In vitro* activity of AcnB and AcnB-G348D.** AcnB catalyzes the reversible conversion of citrate to isocitrate (through the intermediate *cis*-aconitate), a key reaction at the top of the TCA cycle. To ascertain the effects of the G348D mutation on aconitase activity, we measured the kinetic parameters of purified wild-type and G348D mutant proteins for the production of *cis*-aconitate from both directions of the reaction cycle (citrate↔*cis*-aconitate↔isocitrate). The mutant enzyme had a 2.6-fold-lower V_{max} and a slightly lower K_m than those of the wild-type enzyme in the forward reaction and a 3.2-fold-lower V_{max} and 2-fold-higher K_m for the backward reaction (Table 4; Fig. S3). The V_{max} and K_m values for the mutant enzyme in both directions of the reaction were significantly different from those of the wild-type enzyme.

TABLE 4 Kinetic parameters of AcnB activity[a]

	Citrate→*cis*-aconitate		Isocitrate→*cis*-aconitate	
Protein	V_{max} (μmol/min/mg)	K_m (mM)	V_{max} (μmol/min/mg)	K_m (mM)
AcnB	37.1 ± 1.9	21.9 ± 0.7	21.4 ± 0.3	5.0 ± 0.1
AcnB-G348D	14.5 ± 0.2****	16.5 ± 0.4***	6.7 ± 0.3****	10.3 ± 1.2**

[a]Values for V_{max} and K_m were determined from graphs such as those shown in Fig. S3 for conversion of both citrate and isocitrate to *cis*-aconitate. Values represent averages ± standard deviations from a minimum of 4 independent experiments. All values of AcnB-G348D were significantly different from those for AcnB using a 2-tailed unpaired *t* test. ****, *P* value < 0.0001; ***, *P* value = 0.0005; **, *P* value = 0.0073.

Expression of AcnB and AcnB-G348D at different growth phases. Gonococci can grow on glucose, lactate, or pyruvate as a carbon source (37). Morse and colleagues reported that cells grown in glucose-containing medium utilize the Entner-Doudoroff and pentose phosphate pathways, but not the TCA cycle, for ATP production during log-phase (glucose-replete) growth (38–40). Once glucose is depleted, the cells take up extracellular acetate, convert it to citrate (through acetyl coenzyme A [CoA] synthase and citrate synthetase), and feed it into the TCA cycle, where it is acted upon by aconitase. Hebeler and Morse (40) reported that no measurable aconitase activity could be detected in cells under glucose-replete conditions, whereas aconitase activity was observed under glucose-depleted conditions (i.e., stationary-phase growth). These results suggested that aconitase may be regulated in expression as well as in activity during different phases of growth. Therefore, we assessed the protein levels of aconitase in FA19 *acnB*-HA (*acnB* containing a C-terminal hemagglutinin [HA] epitope tag) and FA19 $acnB_{G348D}$-HA as a function of the growth phase in liquid medium. The bacteria were grown in GCB, and starting at $t = 2$ h postinoculation, equivalent OD·ml aliquots were removed every hour, and the levels of AcnB in whole-cell pellets were measured by Western blotting with anti-HA antibody. Wild-type aconitase levels remained fairly constant until the cells entered stationary phase, at which point the protein levels of the enzyme increased by ~2.5-fold (Fig. 6A and B). In contrast, the levels of the G348D mutant aconitase decreased 50% as the cells entered stationary phase (Fig. 6A and B). Analysis of the relative amounts of wild-type and mutant AcnB in bacteria at $t = 2$ h revealed that the mutant aconitase was expressed at 10% of the levels of the wild-type protein (Fig. 6C). Taken together, these data suggest that at stationary phase, when aconitase is required to maintain metabolic competence by utilizing acetate, there is a 50-fold decrease in mutant aconitase protein compared to wild type and a 150-fold decrease in maximal aconitase activity. We conclude from these data that the mutant enzyme acts as a functional knockout, with the sharp plateau in OD_{600} when the cells enter stationary phase reflecting the inability of the bacteria to utilize acetate. Indeed, the growth phenotype of FA19 *penA41* in which *acnB* was insertionally inactivated was very similar to that of FA19 *penA41* $acnB_{G348D}$-HA (Fig. S4).

We next assessed whether the changes in protein expression were the result of changes in *acnB* mRNA transcription. Samples were removed at 2, 3, 7, and 8 h postinoculation, and *acnB* mRNA levels were determined by real-time reverse transcription-PCR (RT-PCR) (Fig. 6D). The mRNA levels for wild-type *acnB* at 2 h were similar to or even higher than those at stationary phase, suggesting that changes in wild-type AcnB expression are posttranscriptional, which would be consistent with the reported role of AcnB as a posttranscriptional regulator in other species of bacteria (41, 42).

RNA-seq analysis of FA19 *penA41* $acnB_{G348D}$ during log-phase growth. To better understand how the mutant $acnB_{G348D}$ allele increases both *in vivo* and *in vitro* fitness, we utilized RNA-seq to determine the differences in the transcriptional profiles of FA19 *penA41* $acnB_{G348D}$ and parental FA19 *penA41* during log-phase growth. We focused on log-phase growth for the following reasons: (i) log phase is where the fitness benefit is most obvious and pronounced and (ii) gonococci in the vaginal tract would be continually exposed to high glucose levels during infection and are unlikely to encounter glucose-depleted conditions in the host (43, 44). Table S2 lists all of the genes that are upregulated and downregulated in FA19 *penA41* $acnB_{G348D}$ compared to FA19 *penA41* during log-phase growth. In total, 66 genes were ≥2-fold upregulated, while 132 genes were ≤2-fold downregulated (in which the Bonferroni-adjusted *P* value was ≤0.05). Strikingly, two-thirds of the genes that were upregulated are involved in energy and carbon metabolism, whereas 43% of the 132 genes that were downregulated were hypothetical genes and another 24% were pilin genes. Taken together, our data suggest that the mutant aconitase increases transcription of a large set of genes that

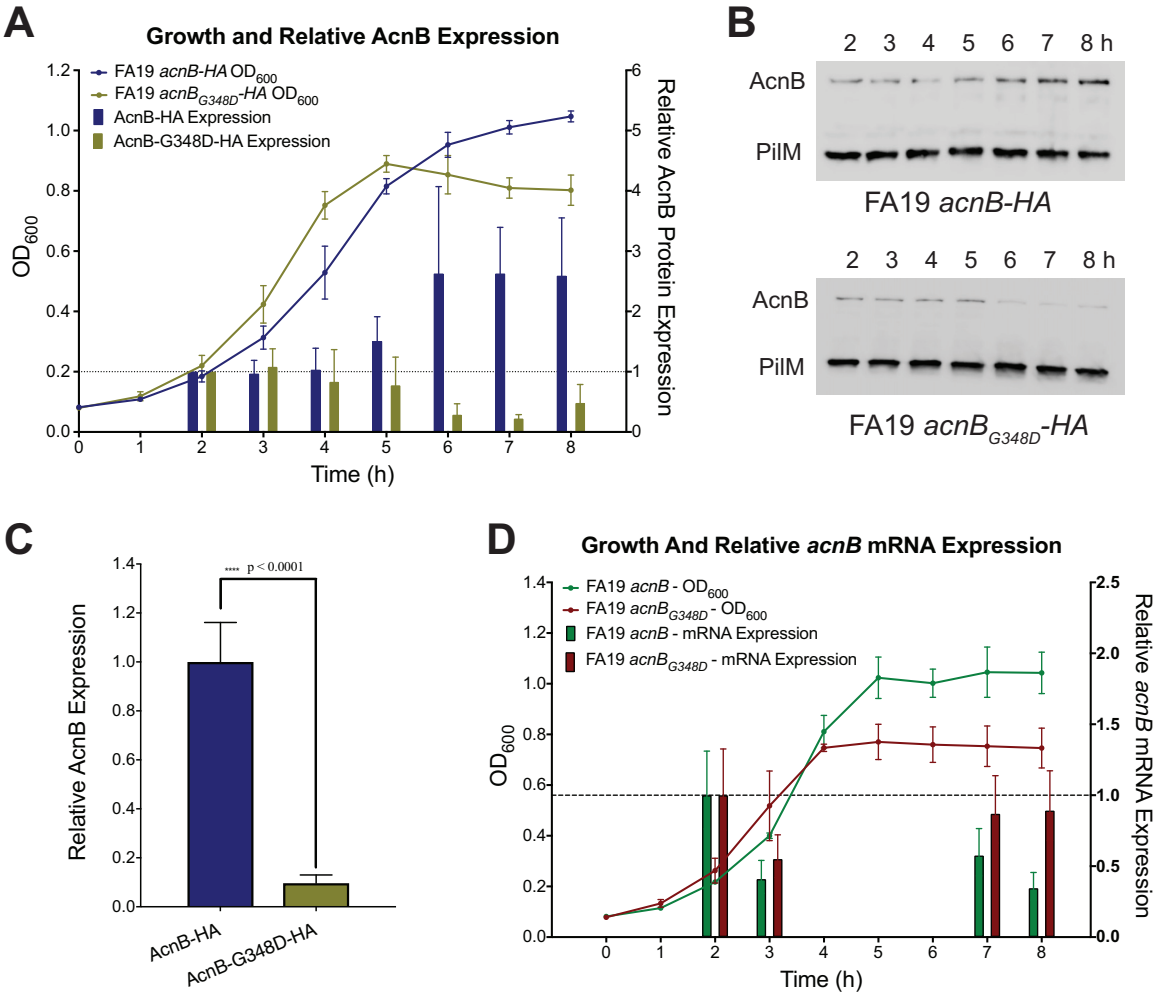

FIG 6 Levels of wild-type and mutant aconitase protein and mRNA during different phases of cell growth. (A) FA19 *acnB*-HA and FA19 $acnB_{G348D}$-HA were grown in culture, and aliquots (equivalent OD_{600} per milliliter) were removed every hour starting at $t = 2$ h. The cells were pelleted, prepared for SDS-PAGE, and then transferred to PVDF membranes for Western blotting with anti-HA antibody. The OD_{600} of the cultures versus time is plotted along with the normalized levels of AcnB-HA proteins (relative to $t = 2$ h). The data plotted are means ± SEM ($n = 4$ for wild-type AcnB and $n = 3$ for AcnB-G348D). (B) Representative Western blots from a single experiment probed with anti-HA and anti-PilM (61) antibodies. (C) Aliquots of cultures of FA19 *acnB*-HA and FA19 $acnB_{G348D}$-HA were removed at $t = 2$ h, and cell lysates were prepared as described above. Protein concentrations of the lysates were determined, and equivalent total proteins of the two lysates were processed for Western blotting. The amounts of wild-type and mutant aconitase were determined, with the levels of wild-type aconitase normalized to 1. Data are the means ± SEM for 6 experiments. (D) Cultures were grown as described for panel A, with samples removed at $t = 2$, 3, 7, and 8 h postinoculation, and mRNA was prepared. Levels of *acnB* mRNA were determined by real-time RT-PCR as described in Materials and Methods. Data are the means ± SEM for 3 independent experiments.

increase the metabolic potential of the cell and thereby alleviate the fitness deficit caused by the mosaic *penA41* gene.

DISCUSSION

Here, we report that the mosaic *penA* alleles from two well-characterized ESC^r clinical isolates, H041 (10) and F89 (12), reduce the fitness of *N. gonorrhoeae* both *in vitro* and *in vivo*. We hypothesized that mosaic *penA* alleles, while increasing ESC resistance, would impart a fitness deficit to a wild-type strain, but in nature, these resistant strains accumulate fitness-increasing mutations that allow the strains to spread (9, 21, 23, 45), as has been shown for other antibiotic-resistant strains (46, 47). We showed that FA19 *penA41*, but not FA19 *penA89*, acquired spontaneous compensatory mutations during coinfections in the female mouse model that markedly increased fitness. We isolated four compensatory mutants, and one of these contained a point mutation in the *acnB* gene encoding the aconitase enzyme that functions in the

TCA cycle. Biochemical analysis showed that the mutation acts as a functional knockout, and our RNA-seq data suggest that the mutation increases expression of a large set of genes involved in energy and carbon metabolism, thereby overcoming the growth defect imparted by the *penA41* allele.

Interestingly, we did not isolate any compensatory mutants of FA19 *penA89* during infection. Acquisition of the *penA89* allele by strain FA19 was more attenuating than the *penA41* allele, as evidenced by the growth phenotype of FA19 *penA89* and the inability to culture any FA19 *penA89* bacteria past day 1 of experimental murine infection. The *penA89* allele contains essentially all of the mutations found in mosaic alleles from cephalosporin-intermediate (Ceph^{i}) strains, with an additional A501P mutation that increases the MIC of ceftriaxone and cefixime for FA19 *penA89* by 5-fold (23). All evidence to date suggests that this additional mutation markedly decreases the essential transpeptidase activity of PBP2, severely compromising cell wall biosynthesis and cell division (PBP2 activity is predicted to be important in septation of dividing cells based on its homology to *Escherichia coli* PBP3 [48]). Based on our findings, we would predict that the *penA89* allele is unlikely to spread, and indeed, there have been no additional infections reported by strains with this allele beyond the three infections (one in France [12] and two in Spain [13]) where the *penA89* allele was first identified. Whether these strains carried compensatory mutations that allowed them to successfully establish infection is not known, but it seems likely. Strain F89, like H041, is resistant to several different antibiotics, and with acquisition of each resistance allele, compensatory mutations may have been selected in parallel to counter fitness costs associated with multiple resistance determinants.

As expected based on the importance of PBP2 in cell division, mosaic PBP2 enzymes with markedly reduced acylation rates impart a growth disadvantage to an antibiotic-susceptible strain of *N. gonorrhoeae*. It is important to note, however, that it is unlikely that the current Cro^{r} isolates that are being identified around the world originated by transformation of a wild-type strain by a mosaic *penA* allele, which then acquired compensatory mutations. Instead, these Cro^{r} strains most likely emerged following transformation of preexisting chromosomally mediated penicillin-resistant (Pen^{r}) strains, which are still common worldwide (49). The Cro^{r} strains harbor all of the other resistance determinants (*mtrR* and *penB*) found in Pen^{r} strains, including the *ponA1* mutation that contributes to penicillin resistance but not ceftriaxone resistance (15, 16, 50). Penicillin was used for over 40 years to treat gonorrhea, and during this time, MICs steadily increased, until in 1986 high-level penicillin resistance necessitated the removal of the antibiotic as a recommended treatment in the United States (5). We suspect that during those 40 years of penicillin treatment, *N. gonorrhoeae* picked up compensatory mutations to improve fitness, thus paving the way for the rapid emergence of Cro^{r} strains following a single transformation event with a mosaic *penA* allele. Work to identify these potential compensatory mutations in resistant clinical isolates is ongoing.

At the initiation of this study, we expected to identify mutations in genes involved in cell wall biosynthesis or division that would compensate for the impaired transpeptidase activity of PBP2. However, with the exception of LV41B, results from growth kinetics and *in vitro* competition assays suggested that the compensatory mutations increased bacterial growth rate and replication. Whole-genome sequence analysis revealed that three of the four *in vivo*-selected compensatory mutant strains contained mutations in genes important to gonococcal physiology and metabolism, and we investigated one of these mutations, $acnB_{G348D}$, in further detail. This mutation decreases both protein levels (by 10- to 50-fold, depending on growth phase) and enzymatic activity (3-fold decrease in V_{max}). When cultured in broth, strains LV41C and FA19 *penA41* $acnB_{G348D}$ both exhibited a rapid log phase of growth followed by a sharp plateau and eventual decline in growth and loss in viability. We suspect that the sharp plateau upon glucose depletion and entrance into stationary phase during *in vitro* growth are a consequence of the marked loss of AcnB protein and activity caused by the G348D mutation, which renders the cell unable to metabolize acetate under glucose-depleted conditions (39, 40, 51).

How mutation of AcnB compensates for the fitness defect displayed by FA19 *penA41* and FA19 *penA89* is not entirely clear. Even though strains harboring an $acnB_{G348D}$ allele showed a sharp plateau during growth in liquid culture upon glucose depletion, when tested *in vivo* these mutants outcompeted the Cro^r parent strain and infected mice for at least 7 days, confirming that there is a fitness benefit associated with this mutant allele. Since it is very unlikely that gonococci would experience glucose depletion during infection in a host, the sharp plateau and eventual decline observed during *in vitro* growth in liquid medium are unlikely to occur during infection. The increase in expression of energy and carbon metabolism-associated genes in log phase (glucose replete) would therefore be sufficient to increase metabolism enough to overcome the negative aspects of harboring a mosaic *penA* allele and thus to confer a fitness advantage over the parental strain, FA19 *penA41*.

The mechanism by which the AcnB-G348D mutant causes such a large change in gene expression is unclear. One possibility is that a change in metabolite composition affects gene transcription, but since aconitase has been reported to be inactive during log-phase growth (40), it is hard to envision that this mechanism is in play. We therefore looked for other possible functions for this protein. It has been reported in other bacteria that when the iron-sulfur network is lost during iron limitation or oxidative stress, aconitase functions as a pleiotropic posttranscriptional regulator by binding to specific mRNA transcripts and regulating their translation (41, 42). Our *in vitro* growth experiments were not done under iron deprivation, but in preliminary *in vitro* experiments, iron limitation did not alter the growth phenotype or increase the *in vitro* fitness of FA19 *penA41* $acnB_{G348D}$. However, it is likely that bacteria are exposed to iron-limiting conditions during infections of the host. Even if aconitase acts as a posttranslational regulator of protein translation, however, that still does not explain such a large difference in gene transcription.

While it is clear that the $acnB_{G348D}$ allele increases fitness, it was not sufficient to bring the level of fitness to that of the compensatory mutant LV41C. We therefore tested whether an additional mutation found in LV41C, a frameshift mutation in the phase-variable *pglG* gene that restores the complete open reading frame, would increase fitness but found no evidence that this mutation alters fitness relative to LV41C. There remain additional untested mutations in the noncoding region downstream of *ftsY*, and it is possible that these mutations alter transcription or transcript stability of the associated gene. This scenario may also explain the fitness advantage of LV41E, which did not contain any mutations in protein-encoding regions.

In summary, here we have demonstrated that two clinically relevant mosaic *penA* alleles, which result in Cro resistance in *N. gonorrhoeae*, impart a fitness deficit compared to their nonmosaic counterparts. *In vivo*, compensatory mutations were readily selected in a Cro^r strain carrying the *penA41* allele that abrogated the fitness disadvantage but not for the more attenuating *penA89* allele. Differences *in vivo* and *in vitro* for the $acnB_{G348D}$ mutation suggest that AcnB may have a yet-undiscovered function(s) that leads to the fitness advantage observed *in vivo*. Ongoing research in this area should lead to novel glimpses into gonococcal metabolism and physiology. Our findings also suggest that ESC resistance may not spread rapidly but that compensatory evolution may allow some ESC^r strains to be maintained in communities and potentially spread. It is doubtful that enough time has elapsed to determine whether Cro^r strains will spread in the human population; global dissemination of resistance to other antibiotics used to treat gonorrhea typically took ~15 to 20 years (5, 10). Continued surveillance for ESC^r strains will be essential to identify whether the compensatory mutations that we have identified in a surrogate infection model are present in ESC^r isolates from natural infections.

MATERIALS AND METHODS

Strains and plasmids. Descriptions of the bacterial strains used in fitness studies are shown in Table S1 in the supplemental material. The antibiotic-susceptible laboratory strain FA19 (52) was used as the background strain for all fitness studies. Streptomycin resistance is required for mouse infection studies (34); therefore, the *rpsL1* gene from FA1090, which encodes a mutant form of ribosomal protein

S12 that confers streptomycin resistance (53), was transformed into strain FA19 by allelic exchange (54). All FA19 strain variants used in this study harbored the *rpsL1* allele.

Strains FA19 *penA41* and FA19 *penA89* are transformants of FA19 in which the wild-type *penA* gene was replaced by the mosaic *penA* alleles from gonococcal strains H041 and F89, respectively, by allelic exchange. Strain FA19 *penA41 cat* was constructed by introducing the ClaI fragment carrying a chloramphenicol acetyltransferase (*cat*) gene from the *Neisseria* chromosomal integration vector pGCC5 (55) into a nonessential intergenic region in FA19 *penA41*. Strains LV41A, LV41B, LV41C, and LV41E are vaginal isolates from *in vivo* competitive infections with strains FA19 and FA19 *penA41*. The $acnB_{G348D}$ mutation from strain LV41C was introduced into strains FA19 *penA41*, FA19, and FA19 *penA89* to create strains FA19 *penA41* $acnB_{G348D}$, FA19 $acnB_{G348D}$, and FA19 *penA89* $acnB_{G348D}$, respectively. The construct used to introduce the $acnB_{G348D}$ allele contained the 3′ end of the $acnB_{G348D}$ gene with a silent NotI restriction site adjacent to the site of the mutation, a Kan^r cassette after the stop codon, and 500 bp downstream of the *acnB* gene. To follow AcnB protein, an analogous construct was made that contained a hexahistidine tag at the very 3′ end of the coding sequence. Transformants were selected on GC agar plates containing 50 μg/ml kanamycin, and mutant and wild-type *acnB* transformants were identified by PCR amplification and digestion with NotI and verified by Sanger sequencing.

All gonococcal strains were propagated on solid GCB agar containing Kellogg's supplement I (56) and 12 μM $Fe(NO_3)_3$ for 18 to 20 h at 37°C in a 4% CO_2-enriched atmosphere. Passage from frozen stocks was minimized to reduce the risk of acquiring secondary mutations. For competitive infections and cocultures, GCB agar plates containing antibiotic selection were used to isolate the mutants as follows: ceftriaxone, 0.125 μg/ml for FA19 *penA41*, LV41A, LV41B, LV41C, and LV41E and 0.008 μg/ml for FA19 *penA89*; chloramphenicol, 0.5 μg/ml for FA19 *penA41 cat*; kanamycin, 50 μg/ml for FA19 *penA41* $acnB_{G438D}$ and FA19 *penA89* $acnB_{G348D}$. Streptomycin (100 μg/ml) was included in the GCB agar plates used for vaginal cultures.

Bacterial growth. Bacterial colonies with nonpiliated morphology were harvested with a sterile swab and inoculated into GCB (per liter: 15 g protease peptone 3, 4 g K_2HPO_4, dibasic, 1 g KH_2PO_4, 5 g NaCl) supplemented with Kellogg's supplement I (56), 12 μM $Fe(NO_3)_3$, and 5 mM $NaHCO_3$. Cultures were shaken at 220 rpm at 37°C, and bacterial growth was assessed by measuring the OD_{600} at hourly intervals for a total of 8 h. Aliquots were also quantitatively cultured every 2 h on GCB agar plates with and without antibiotic selection to determine the number of CFU per milliliter of total bacteria or mutant bacteria, respectively. Experiments were repeated six times, and data were combined and analyzed using a repeated-measures 2-way analysis of variance (ANOVA) with Tukey's multiple comparisons. Differences in growth rate were measured by comparing the average numbers of minutes that it took to reach an OD_{600} of 0.8 for each strain as previously described (26). Results were compared using a one-way analysis of variance to determine overall significance followed by Student's *t* test to determine significance between individual strains.

Antimicrobial susceptibility testing. The MICs of Cro, penicillin G, erythromycin, ciprofloxacin, and chloramphenicol were determined by agar dilution as described previously (23).

***In vitro* competition experiments.** Competitive coculture was used to compare the fitness of Cro^s or Cro^r parent strains with those of mutant strains FA19 *penA41* and FA19 *penA89* or the *in vivo*-selected compensatory mutants of FA19 *penA41*. Bacteria were harvested from GCB agar plates and suspended in liquid GCB, and suspensions were adjusted to an OD_{600} of 0.8. Equal volumes of the suspensions of each strain to be compared were inoculated into supplemented GC broth with 5 mM $NaHCO_3$ (starting OD_{600} of 0.08), and cultures were shaken at 220 rpm at 37°C. Aliquots were cultured quantitatively at the time of inoculation ($t = 0$) and every 2 h thereafter on GCB agar with no antibiotics (total CFU) and GCB agar with antibiotic selection. The CI was determined hourly for 8 h, whereby the ratio of mutant to wild-type bacteria at output was divided by the ratio of mutant to wild-type bacteria at input (57). Experiments were conducted three times, and the geometric mean CI at each time point was determined.

Competitive murine infections. All animal experiments were conducted at the Uniformed Services University of the Health Sciences, a facility fully accredited by the Association for Assessment and Accreditation of Laboratory Animal Care, under a protocol that was approved by the university's Institutional Animal Care and Use Committee. Female BALB/c mice (6 to 8 weeks old, National Cancer Institute) were treated subcutaneously with 0.5 mg of either water-soluble β-estradiol (catalogue no. E-4389; Sigma-Aldrich, St. Louis, MO) or oil-soluble β-estradiol 3-benzoate (catalogue no. E-8515; Sigma-Aldrich) suspended in sesame oil when competing compensatory mutant strains against parent and wild-type strains. In all experiments, β-estradiol was given on days -2, 0, and $+2$ of infection. Mice were also given streptomycin sulfate, vancomycin, and trimethoprim to reduce the overgrowth of commensal flora as described previously (34). Two days after the first injection of β-estradiol, mice were inoculated intravaginally with 20 μl of a mixed bacterial suspension containing 1×10^6 to 2×10^6 CFU of each strain ($n = 4$ to 8 mice per experiment). Vaginal swabs were collected on days 1, 3, 5, and 7 postinoculation and suspended in 1 ml of phosphate-buffered saline (PBS). Equal volumes of vaginal swab suspensions were cultured quantitatively on GCB agar with streptomycin (100 μg/ml) (total CFU) and GCB agar with streptomycin plus the appropriate selection as described above (mutant CFU). A CI was determined whereby the ratio of mutant to wild-type bacteria in vaginal cultures at each individual time point was divided by the ratio of mutant to wild-type bacteria in the inoculum. For those cultures from which only one strain was recovered, the limit of detection (4 CFU) was used as the number of CFU for the strain that was not isolated when calculating the CI. Experiments were conducted two or three times for each mixture.

Genomic resequencing. Genomic DNA was extracted using the Promega Wizard genomic DNA purification kit (Promega, Madison, WI) according to the manufacturer's protocol using bacteria grown to mid-log phase in supplemented GCB. The extracted DNA was rehydrated overnight, and the DNA was quantified using a NanoDrop 1000 spectrophotometer. A mate-pair library was constructed using Nextera XT standard kits (Illumina FC-121-1024 and FC-121-1001) and prepared for emulsion-based amplification and paired-end sequencing. Illumina MiSeq 2500 genomic DNA paired-end sequencing was conducted by the Tufts University Core Facility using a v2 flow cell paired-end 250-base (PE250) format. Each read was 251 bases with two reads per insert plus a barcode. The insert for PE250 with Nextera XT ranges from 500 bp to 1,300 bp, with the average/peak size range around 800 bp. Data were analyzed using CLC Genomics Workbench version 6.0.4 against the recently sequenced FA19 genome sequence (58). The threshold to be flagged as a mutation was set to 85% mutation frequency of all aligned reads.

Coverage (number of mapped bases/number of bases in FA19) for the different strains ranged from 360 for LV41B to 483 for LV41A, with a fairly even distribution across the genome. No deletions larger than 3 nucleotides (e.g., the codon deletion in *mleN*) were observed for any of the strains; however, there were 10 regions of ~100 bp in length in the resequencing data for all of the resequenced strains that had low coverage (<7 reads). These regions were in or nearby PROKKA 0283, 0477, 0600, 0814, 0839, 1584, 1966, 1990, 2035, and 2217. Primers were made to these regions, and DNA surrounding the low-coverage regions was amplified by PCR and sequenced by Sanger sequencing. In all cases, the sequences were identical to FA19.

Aconitase kinetics. The aconitase gene was amplified from either FA19 or LV41C by PCR and cloned into pMALC2KV, which fused the gene in frame with hexahistidine-tagged maltose-binding protein and an intervening tobacco etch virus (TEV) protease site. Following expression in *E. coli* and purification on a Ni^{2+}-nitrilotriacetic acid (NTA) column, the fusion proteins were cleaved with His-TEV protease and run again over the column to retain any uncleaved protein and His-TEV and allow the purified enzymes to flow through the column. The proteins were concentrated and stored at −80°C. For enzymatic analysis, the thawed enzyme was reactivated immediately prior to assay by incubation on ice with 5 μl 0.5 M dithiothreitol (DTT), 0.5 μl 20 mM Na_2S, and 0.5 μl 20 mM $(NH_4)2Fe(SO_4)_2$ under nitrogen (59). After 30 min, the tube was opened and immediately diluted into 100 μl buffer containing a range of citrate or isocitrate concentrations, and the increase in OD_{240} was monitored on a BMG PolarStar Omega plate reader in UV-clear microtiter plates. The slopes of each reaction within the first minute were used to calculate the initial velocity of the enzymes.

RNA extraction, RT-PCR, and quantitative PCR (qPCR). The appropriate strains were grown in liquid GC broth medium with glucose as the main carbon source. The equivalent of 10 ml of cells at an OD_{600} of 0.18 was removed at 2 and 3 h (log phase) and at 7 and 8 h (stationary phase) of growth, and the bacteria were collected by centrifugation, resuspended in RNAlater solution, and stored at 4°C. Total RNA from the cells was extracted the next day using the Bio-Rad Aurum total RNA minikit and eluted in 40 μl RNase-free water. One microliter of RNasin (RNase inhibitor; Promega, Madison, WI) was added to the extracted RNA, and the total RNA concentration was determined using a NanoDrop reader. To remove DNA contamination, 1 μg of total RNA was digested for approximately 40 min at 37°C with 1 unit of RQ1 RNase-free DNase (Promega). The DNase was inactivated using the supplied stop solution at 65°C for 10 min.

cDNA was generated from purified total RNA using the Bio-Rad iScript reverse transcription supermix (Bio-Rad, Hercules, CA). Real-time qPCR was performed using the Bio-Rad Sso Advanced Universal SYBR green supermix and the Bio-Rad CFX96 Touch real-time PCR detection system. Fold change was determined using the threshold cycle ($2^{-\Delta\Delta CT}$) method (60), with 16S rRNA as the reference gene. RNA reference samples were diluted 1:50,000 using RNase-free water.

Western blotting and electrophoresis. The appropriate strains were prepared for growth in supplemented liquid GCB, and aliquots were taken hourly starting at 2 h postinoculation. The equivalent of 1 ml of cells at an OD_{600} of 0.18 (i.e., 0.18 OD per ml) was pelleted, the supernatant was aspirated, and the samples were frozen at −20°C if not used immediately. Pellets were resuspended in 100 μl fresh 1× Laemmli sample buffer (0.07 M Tris-HCl, pH 6.8, 10% glycerol, 5% β-mercaptoethanol, 1.05% SDS, dyed with bromophenol blue) and boiled for 5 min. Samples were centrifuged briefly, and equal volumes of protein were loaded and resolved on a 10% polyacrylamide SDS-PAGE gel.

The proteins were transferred to a polyvinylidene difluoride (PVDF) membrane and blocked in PBS-Tween (PBS with 0.1% Tween 100) containing 5% nonfat dry milk (NFDM) for 1 h at room temperature on a shaker table. The membrane was incubated in PBS-Tween containing 2.5% NFDM and 1:10,000 rabbit PilM antibody (61) for 1 h at room temperature. The membrane was then washed four times for 9 min each in fresh PBS-Tween and then incubated in PBS-Tween containing 2.5% NFDM, 1:1,000 3F10 (mouse HA antibody conjugated with horseradish peroxidase [HRP]), and 1:20,000 goat anti-rabbit HRP-conjugated antibody for 1 h at room temperature. The membrane was washed again as previously described and then incubated for 2 min with Bio-Rad enhanced chemiluminescence (ECL) reagents and imaged using the Bio-Rad ChemiDoc Touch imager. PilM was used as an internal loading control because its expression does not appear to change in different phases of growth; however, it was not used to normalize protein expression between strains because its expression appears to vary between strains.

RNA extraction, purification, library preparation, and RNA-seq. RNA-seq was carried out for FA19 *penA41* and FA19 *penA41* $acnB_{G348D}$ from three separate cultures on different days for each strain. Bacteria were streaked from frozen stocks onto GCB agar plates and grown for 20 h at 37°C in a 4% CO_2 atmosphere. Liquid cultures were prepared as described above for the *in vitro* growth curves and grown until the cells reached log phase (OD_{600} of ~0.4 to 0.5). Three milliliters was removed, and the cells were

pelleted, resuspended in RNAlater solution, and stored overnight at 4°C. The next morning, total RNA was isolated using the Qiagen RNeasy minikit (Qiagen, Carlsbad, CA), contaminating DNA was removed by DNase digestion using the Invitrogen Turbo DNA-free kit, and the RNA was reisolated using the RNeasy minikit. rRNA was removed by 2 successive rounds of treatment with the Life Technologies MICROBExpress mRNA prep kit (Thermo Fisher, Grand Island, NY), and the mRNA was recovered with the Qiagen RNeasy MinElute cleanup kit. All mRNA samples were analyzed using the Agilent high-sensitivity ScreenTape system to determine quality (Agilent, Santa Clara, CA) and by a NanoDrop spectrophotometer to assess quantity. Libraries were prepared from a minimum of three separate cultures of each strain using the Illumina TruSeq high-sample (HS) protocol (Illumina, San Diego, CA). First- and second-strand cDNAs were synthesized using AMPure XP magnetic beads, first- and second-strand master mixes, and SuperScript II reverse transcriptase. End repair, 3′ end adenylation, adapter ligation, and DNA fragment enrichment were all performed according to the TruSeq protocol. The quality of the DNA libraries was analyzed by the Agilent high-sensitivity ScreenTape system, and the concentrations were determined using the Qubit double-stranded DNA (dsDNA) HS assay kit (Thermo Fisher, Grand Island, NY). Equimolar DNA amounts of each library were pooled and prepared for sequencing on the Illumina NextSeq 500 system according to the manufacturer's system guide. Run parameters and data were collected using Illumina BaseSpace.

The data were mapped to the FA19 genomic sequence with the CLC Genomics Workbench software package (version 11.0; Qiagen) using the RNA-seq analysis command, with mapping options of mismatch cost = 2, insertion cost = 3, deletion cost = 3, length fraction = 0.8, similarity option = 0.8, and the maximum number of hits for a read = 3. Between 85 and 90% of reads for each alignment had a reads per kilobase per million (RPKM) of >5. To determine differentially expressed genes, the differential expression for RNA-seq command was run. Table S2 lists all of the genes with a Bonferroni-adjusted *P* value of ≤0.05 with a differential expression of ≥2-fold higher or lower.

Accession number(s). The .fastq and aligned .bam files can be obtained from the Sequence Read Archive under accession number SRP132214.

SUPPLEMENTAL MATERIAL

Supplemental material for this article may be found at https://doi.org/10.1128/mBio.01905-17.

FIG S1, EPS file, 0.1 MB.
FIG S2, EPS file, 2.2 MB.
FIG S3, EPS file, 0.1 MB.
FIG S4, EPS file, 0.2 MB.
FIG S5, EPS file, 0.1 MB.
TABLE S1, DOCX file, 0.02 MB.
TABLE S2, DOCX file, 0.03 MB.

ACKNOWLEDGMENTS

We thank Cara Olsen for help with statistical analyses and Ian McDonald for helping with the aconitase assays. We also thank William Shafer at Emory University for helpful discussions and critical review of the manuscript.

The contents of this article are solely the responsibility of the authors and do not necessarily represent the official views of the Uniformed Services University of the Health Sciences, the Department of Defense, or the University of North Carolina.

This work was supported by a grant from the National Institute of Allergy and Infectious Diseases, U19 AI113170 (A.E.J. and R.A.N.), and an intramural grant (MIC73-2493) from the Uniformed Services University (A.E.J.). The funders had no role in study design, data collection and interpretation, or the decision to submit the work for publication.

REFERENCES

1. Newman L, Rowley J, Vander Hoorn S, Wijesooriya NS, Unemo M, Low N, Stevens G, Gottlieb S, Kiarie J, Temmerman M. 2015. Global estimates of the prevalence and incidence of four curable sexually transmitted infections in 2012 based on systematic review and global reporting. PLoS One 10:e0143304. https://doi.org/10.1371/journal.pone.0143304.
2. Hook EW, Handsfield HH. 1999. Gonococcal infections in the adult, p 451–466. *In* Holmes KK, Sparling PF, Mardh P-A, Stamm WS, Piot P, Wasserheit JN (ed), Sexually transmitted infections, 3rd ed. McGraw-Hill, New York, NY.
3. Jarvis GA, Chang TL. 2012. Modulation of HIV transmission by *Neisseria gonorrhoeae*: molecular and immunological aspects. Curr HIV Res 10:211–217. https://doi.org/10.2174/157016212800618138.
4. Cohen MS, Hoffman IF, Royce RA, Kazembe P, Dyer JR, Daly CC, Zimba D, Vernazza PL, Maida M, Fiscus SA, Eron JJ, Jr. 1997. Reduction of concentration of HIV-1 in semen after treatment of urethritis: implications for prevention of sexual transmission of HIV-1. AIDSCAP Malawi Research Group. Lancet 349:1868–1873. https://doi.org/10.1016/S0140-6736(97)02190-9.
5. Unemo M, Nicholas RA, Jerse AE, Davies C, Shafer WM. 2014. Molecular mechanisms of antibiotic resistance expressed by the pathogenic *Ne-*

ustria, p 161–192. *In* Davies JK, Kahler CM (ed), Pathogenic *Neisseria*, 2nd ed. Caister Academic Press, Poole, United Kingdom.
6. Wi T, Lahra MM, Ndowa F, Bala M, Dillon JR, Ramon-Pardo P, Eremin SR, Bolan G, Unemo M. 2017. Antimicrobial resistance in *Neisseria gonorrhoeae*: global surveillance and a call for international collaborative action. PLoS Med 14:e1002344. https://doi.org/10.1371/journal.pmed.1002344.
7. CDC. 2007. Update to CDC's sexually transmitted diseases treatment guidelines, 2006: fluoroquinolones no longer recommended for treatment of gonococcal infections. MMWR Morb Mortal Wkly Rep 56:332–336.
8. CDC. 2012. Update to CDC's sexually transmitted diseases treatment guidelines, 2010: oral cephalosporins no longer a recommended treatment for gonococcal infections. MMWR Morb Mortal Wkly Rep 61:590–594.
9. Unemo M. 2015. Current and future antimicrobial treatment of gonorrhoea—the rapidly evolving *Neisseria gonorrhoeae* continues to challenge. BMC Infect Dis 15:364. https://doi.org/10.1186/s12879-015-1029-2.
10. Ohnishi M, Golparian D, Shimuta K, Saika T, Hoshina S, Iwasaku K, Nakayama SI, Kitawaki J, Unemo M. 2011. Is *Neisseria gonorrhoeae* initiating a future era of untreatable gonorrhea? Detailed characterization of the first high-level ceftriaxone resistant strain. Antimicrob Agents Chemother 55:3538–3545. https://doi.org/10.1128/AAC.00325-11.
11. Ohnishi M, Saika T, Hoshina S, Iwasaku K, Nakayama S, Watanabe H, Kitawaki J. 2011. Ceftriaxone-resistant *Neisseria gonorrhoeae*, Japan. Emerg Infect Dis 17:148–149. https://doi.org/10.3201/eid1701.100397.
12. Unemo M, Golparian D, Nicholas R, Ohnishi M, Gallay A, Sednaoui P. 2012. High-level cefixime- and ceftriaxone-resistant *N. gonorrhoeae* in France: novel *penA* mosaic allele in a successful international clone causes treatment failure. Antimicrob Agents Chemother 56:1273–1280. https://doi.org/10.1128/AAC.05760-11.
13. Cámara J, Serra J, Ayats J, Bastida T, Carnicer-Pont D, Andreu A, Ardanuy C. 2012. Molecular characterization of two high-level ceftriaxone-resistant *Neisseria gonorrhoeae* isolates detected in Catalonia, Spain. J Antimicrob Chemother 67:1858–1860. https://doi.org/10.1093/jac/dks162.
14. Ito M, Deguchi T, Mizutani KS, Yasuda M, Yokoi S, Ito S, Takahashi Y, Ishihara S, Kawamura Y, Ezaki T. 2005. Emergence and spread of *Neisseria gonorrhoeae* clinical isolates harboring mosaic-like structure of penicillin-binding protein 2 in central Japan. Antimicrob Agents Chemother 49:137–143. https://doi.org/10.1128/AAC.49.1.137-143.2005.
15. Zhao S, Duncan M, Tomberg J, Davies C, Unemo M, Nicholas RA. 2009. Genetics of chromosomally mediated intermediate resistance to ceftriaxone and cefixime in *Neisseria gonorrhoeae*. Antimicrob Agents Chemother 53:3744–3751. https://doi.org/10.1128/AAC.00304-09.
16. Lindberg R, Fredlund H, Nicholas RA, Unemo M. 2007. *Neisseria gonorrhoeae* isolates with reduced susceptibility to cefixime and ceftriaxone: association with genetic polymorphisms in *penA*, *mtrR*, *porB1b*, and *ponA*. Antimicrob Agents Chemother 51:2117–2122. https://doi.org/10.1128/AAC.01604-06.
17. Hagman KE, Pan W, Spratt BG, Balthazar JT, Judd RC, Shafer WM. 1995. Resistance of *Neisseria gonorrhoeae* to antimicrobial hydrophobic agents is modulated by the *mtrRCDE* efflux system. Microbiology 141:611–622. https://doi.org/10.1099/13500872-141-3-611.
18. Olesky M, Hobbs M, Nicholas RA. 2002. Identification and analysis of amino acid mutations in porin IB that mediate intermediate-level resistance to penicillin and tetracycline in *Neisseria gonorrhoeae*. Antimicrob Agents Chemother 46:2811–2820. https://doi.org/10.1128/AAC.46.9.2811-2820.2002.
19. Gill MJ, Simjee S, Al-Hattawi K, Robertson BD, Easmon CS, Ison CA. 1998. Gonococcal resistance to β-lactams and tetracycline involves mutation in loop 3 of the porin encoded at the *penB* locus. Antimicrob Agents Chemother 42:2799–2803.
20. Olesky M, Zhao S, Rosenberg RL, Nicholas RA. 2006. Porin-mediated antibiotic resistance in *Neisseria gonorrhoeae*: ion, solute, and antibiotic permeation through PIB proteins with penB mutations. J Bacteriol 188:2300–2308. https://doi.org/10.1128/JB.188.7.2300-2308.2006.
21. Tomberg J, Unemo M, Ohnishi M, Davies C, Nicholas RA. 2013. Identification of amino acids conferring high-level resistance to expanded-spectrum cephalosporins in the *penA* gene from *Neisseria gonorrhoeae* strain H041. Antimicrob Agents Chemother 57:3029–3036. https://doi.org/10.1128/AAC.00093-13.
22. Tomberg J, Unemo M, Davies C, Nicholas RA. 2010. Molecular and structural analysis of mosaic variants of penicillin-binding protein 2 conferring decreased susceptibility to expanded-spectrum cephalosporins in *Neisseria gonorrhoeae*: role of epistatic mutations. Biochemistry 49:8062–8070. https://doi.org/10.1021/bi101167x.
23. Tomberg J, Fedarovich A, Vincent LR, Jerse AE, Unemo M, Davies C, Nicholas RA. 2017. Alanine-501 mutations in penicillin-binding protein 2 from *Neisseria gonorrhoeae*: structure, function, and effects on cephalosporin resistance and biological fitness. Biochemistry 56:1140–1150. https://doi.org/10.1021/acs.biochem.6b01030.
24. Andersson DI, Hughes D. 2010. Antibiotic resistance and its cost: is it possible to reverse resistance? Nat Rev Microbiol 8:260–271. https://doi.org/10.1038/nrmicro2319.
25. Warner DM, Shafer WM, Jerse AE. 2008. Clinically relevant mutations that cause derepression of the *Neisseria gonorrhoeae* MtrC-MtrD-MtrE efflux pump system confer different levels of antimicrobial resistance and in vivo fitness. Mol Microbiol 70:462–478. https://doi.org/10.1111/j.1365-2958.2008.06424.x.
26. Kunz AN, Begum AA, Wu H, D'Ambrozio JA, Robinson JM, Shafer WM, Bash MC, Jerse AE. 2012. Impact of fluoroquinolone resistance mutations on gonococcal fitness and in vivo selection for compensatory mutations. J Infect Dis 205:1821–1829. https://doi.org/10.1093/infdis/jis277.
27. D'Ambrozio JA. 2015. Insights into the enhanced in vivo fitness of *Neisseria gonorrhoeae* driven by a fluoroquinolone resistance-conferring mutant DNA gyrase. PhD dissertation. Uniformed Services University of the Health Sciences, Bethesda, MD.
28. Trzcinski K, Thompson CM, Gilbey AM, Dowson CG, Lipsitch M. 2006. Incremental increase in fitness cost with increased beta-lactam resistance in pneumococci evaluated by competition in an infant rat nasal colonization model. J Infect Dis 193:1296–1303. https://doi.org/10.1086/501367.
29. Albarracín Orio AG, Piñas GE, Cortes PR, Cian MB, Echenique J. 2011. Compensatory evolution of PBP mutations restores the fitness cost imposed by beta-lactam resistance in *Streptococcus pneumoniae*. PLoS Pathog 7:e1002000. https://doi.org/10.1371/journal.ppat.1002000.
30. Haenni M, Moreillon P. 2008. Fitness cost and impaired survival in penicillin-resistant *Streptococcus gordonii* isolates selected in the laboratory. Antimicrob Agents Chemother 52:337–339. https://doi.org/10.1128/AAC.00939-07.
31. Grad YH, Kirkcaldy RD, Trees D, Dordel J, Harris SR, Goldstein E, Weinstock H, Parkhill J, Hanage WP, Bentley S, Lipsitch M. 2014. Genomic epidemiology of *Neisseria gonorrhoeae* with reduced susceptibility to cefixime in the USA: a retrospective observational study. Lancet Infect Dis 14:220–226. https://doi.org/10.1016/S1473-3099(13)70693-5.
32. Andersson DI. 2003. Persistence of antibiotic resistant bacteria. Curr Opin Microbiol 6:452–456. https://doi.org/10.1016/j.mib.2003.09.001.
33. Warner DM, Folster JP, Shafer WM, Jerse AE. 2007. Regulation of the MtrC-MtrD-MtrE efflux-pump system modulates the in vivo fitness of *Neisseria gonorrhoeae*. J Infect Dis 196:1804–1812. https://doi.org/10.1086/522964.
34. Jerse AE, Wu H, Packiam M, Vonck RA, Begum AA, Garvin LE. 2011. Estradiol-treated female mice as surrogate hosts for *Neisseria gonorrhoeae* genital tract infections. Front Microbiol 2:107. https://doi.org/10.3389/fmicb.2011.00107.
35. Wei Y, Guffanti AA, Ito M, Krulwich TA. 2000. *Bacillus subtilis* YqkI is a novel malic/Na^+-lactate antiporter that enhances growth on malate at low protonmotive force. J Biol Chem 275:30287–30292. https://doi.org/10.1074/jbc.M001112200.
36. Anonsen JH, Vik Å, Børud B, Viburiene R, Aas FE, Kidd SW, Aspholm M, Koomey M. 2015. Characterization of a unique tetrasaccharide and distinct glycoproteome in the O-linked protein glycosylation system of *Neisseria elongata* subsp. *glycolytica*. J Bacteriol 198:256–267. https://doi.org/10.1128/JB.00620-15.
37. Morse SA. 1978. The biology of the gonococcus. CRC Crit Rev Microbiol 7:93–189. https://doi.org/10.3109/10408417909083071.
38. Morse SA. 1979. *Neisseria gonorrhoeae*: physiology and metabolism. Sex Transm Dis 6:28–37. https://doi.org/10.1097/00007435-197901000-00009.
39. Morse SA, Stein S, Hines J. 1974. Glucose metabolism in *Neisseria gonorrhoeae*. J Bacteriol 120:702–714.
40. Hebeler BH, Morse SA. 1976. Physiology and metabolism of pathogenic Neisseria: tricarboxylic acid cycle activity in *Neisseria gonorrhoeae*. J Bacteriol 128:192–201.
41. Tang Y, Guest JR. 1999. Direct evidence for mRNA binding and post-

transcriptional regulation by *Escherichia coli* aconitases. Microbiology 145:3069–3079. https://doi.org/10.1099/00221287-145-11-3069.
42. Austin CM, Wang G, Maier RJ. 2015. Aconitase functions as a pleiotropic posttranscriptional regulator in Helicobacter pylori. J Bacteriol 197: 3076–3086. https://doi.org/10.1128/JB.00529-15.
43. Exley RM, Wu H, Shaw J, Schneider MC, Smith H, Jerse AE, Tang CM. 2007. Lactate acquisition promotes successful colonization of the murine genital tract by *Neisseria gonorrhoeae*. Infect Immun 75:1318–1324. https://doi.org/10.1128/IAI.01530-06.
44. Owen DH, Katz DF. 1999. A vaginal fluid simulant. Contraception 59: 91–95. https://doi.org/10.1016/S0010-7824(99)00010-4.
45. Unemo M, Nicholas RA. 2012. Emergence of multidrug-resistant, extensively drug-resistant and untreatable gonorrhea. Future Microbiol 7:1401–1422. https://doi.org/10.2217/fmb.12.117.
46. Comas I, Borrell S, Roetzer A, Rose G, Malla B, Kato-Maeda M, Galagan J, Niemann S, Gagneux S. 2011. Whole-genome sequencing of rifampicin-resistant *Mycobacterium tuberculosis* strains identifies compensatory mutations in RNA polymerase genes. Nat Genet 44:106–110. https://doi.org/10.1038/ng.1038.
47. Bæk KT, Thøgersen L, Mogenssen RG, Mellergaard M, Thomsen LE, Petersen A, Skov S, Cameron DR, Peleg AY, Frees D. 2015. Stepwise decrease in daptomycin susceptibility in clinical *Staphylococcus aureus* isolates associated with an initial mutation in *rpoB* and a compensatory inactivation of the *clpX* gene. Antimicrob Agents Chemother 59: 6983–6991. https://doi.org/10.1128/AAC.01303-15.
48. Suzuki H, Nishimura Y, Hirota Y. 1978. On the process of cellular division in Escherichia coli: a series of mutants of E. coli altered in the penicillin-binding proteins. Proc Natl Acad Sci U S A 75:664–668. https://doi.org/10.1073/pnas.75.2.664.
49. Kirkcaldy RD, Harvey A, Papp JR, Del Rio C, Soge OO, Holmes KK, Hook EW, III, Kubin G, Riedel S, Zenilman J, Pettus K, Sanders T, Sharpe S, Torrone E. 2016. *Neisseria gonorrhoeae* antimicrobial susceptibility surveillance—the Gonococcal Isolate Surveillance Project, 27 sites, United States, 2014. MMWR Surveill Summ 65:1–19. https://doi.org/10.15585/mmwr.ss6507a1.
50. Ropp PA, Hu M, Olesky M, Nicholas RA. 2002. Mutations in *ponA*, the gene encoding penicillin-binding protein 1, and a novel locus, *penC*, are required for high-level chromosomally mediated penicillin resistance in *Neisseria gonorrhoeae*. Antimicrob Agents Chemother 46:769–777. https://doi.org/10.1128/AAC.46.3.769-777.2002.
51. Morse SA, Miller RD, Hebeler BH. 1977. Physiology and metabolism of *Neisseria gonorrhoeae*, p 213–254. *In* Roberts RB (ed), The gonococcus. John Wiley & Sons, New York, NY.
52. Maness MJ, Sparling PF. 1973. Multiple antibiotic resistance due to a single mutation in *Neisseria gonorrhoeae*. J Infect Dis 128:321–330. https://doi.org/10.1093/infdis/128.3.321.
53. Sparling PF, Modolell J, Takeda Y, Davis BD. 1968. Ribosomes from *Escherichia coli* merodiploids heterozygous for resistance to streptomycin and to spectinomycin. J Mol Biol 37:407–421. https://doi.org/10.1016/0022-2836(68)90111-3.
54. Gunn JS, Stein DC. 1996. Use of a non-selective transformation technique to construct a multiply restriction/modification-deficient mutant of *Neisseria gonorrhoeae*. Mol Gen Genet 251:509–517. https://doi.org/10.1007/BF02173639.
55. Mehr IJ, Seifert HS. 1997. Random shuttle mutagenesis: gonococcal mutants deficient in pilin antigenic variation. Mol Microbiol 23: 1121–1131. https://doi.org/10.1046/j.1365-2958.1997.2971660.x.
56. Kellogg DS, Peacock WL, Deacon WE, Browh L, Perkle CI. 1963. *Neisseria gonorrhoeae*. I. Virulence genetically linked to colonial variation. J Bacteriol 85:1274–1279.
57. Wu H, Jerse AE. 2006. Alpha-2,3-sialyltransferase enhances *Neisseria gonorrhoeae* survival during experimental murine genital tract infection. Infect Immun 74:4094–4103. https://doi.org/10.1128/IAI.00433-06.
58. Abrams AJ, Trees DL, Nicholas RA. 2015. Complete genome sequences of three *Neisseria gonorrhoeae* laboratory reference strains, determined using PacBio single-molecule real-time technology. Genome Announc 3:e01052-15. https://doi.org/10.1128/genomeA.01052-15.
59. Hausladen A, Fridovich I. 1996. Measuring nitric oxide and superoxide: rate constants for aconitase reactivity. Methods Enzymol 269:37–41.
60. Lewis AM, Rice KC. 2016. Quantitative real-time PCR (qPCR) workflow for analyzing *Staphylococcus aureus* gene expression. Methods Mol Biol 1373:143–154. https://doi.org/10.1007/7651_2014_193.
61. Nandi S, Swanson S, Tomberg J, Nicholas RA. 2015. Diffusion of antibiotics through the PilQ secretin in *Neisseria gonorrhoeae* occurs through the immature, sodium dodecyl sulfate-labile form. J Bacteriol 197: 1308–1321. https://doi.org/10.1128/JB.02628-14.